Monitoring the Postural Stability of Planar Bipedal Robots using the Moment-Height Stability Measure

Mansoor Alghooneh[1], Amir Takhmar[2], and S. Ali. A. Moosavian[3]

[1] Research Assistant, Nonlinear Systems Research Laboratory (NSRL), Department of Mechanical and Manufacturing Engineering, University of Manitoba, Winnipeg, Manitoba, Canada, email: umalghoo@cc.umanitoba.ca; alghooneh@gmail.com.

[2] Research Assistant, Department of Electrical and Computer Engineering, University of Western Ontario, London, Ontario, Canada, email: amir.takhmar@gmail.com.

[3] Full Professor, Advanced Robotics & Automated Systems (ARAS) Laboratory, Department of Mechanical Engineering, K. N. Toosi University of Technology, Tehran, Iran, email: moosavian@kntu.ac.ir.

Submitted: Apr. 11, 2012 ***Accepted: May 14, 2012*** ***Published: June 1, 2012***

Abstract - Robotics researchers have studied the stability maintenance requirements of bipedal robots since they are inherently unstable. An accurate postural stability measure is required to monitor their dynamic equilibrium conditions. In this article, the novel Moment-Height Stability (MHS) measure, which has previously been developed for monitoring the postural stability of wheeled mobile robots, is developed for that of bipedal robots. The performance of the MHS is evaluated with that of the well-known postural stability measure Zero-Moment Point (ZMP). The MHS and the ZMP are applied to two types of manoeuvres of a planar bipedal robot, consisting of standing up and swinging forward. Simulation results reveal that both the ZMP and the MHS predict the same instant for the occurrence of postural instability for the biped; the MHS warns the biped that the potential of postural instability amplifies once the overall height

Two types of trajectories for the biped namely standing up and swinging forward are designed using the compensation method [15]. The MHS and the ZMP are implemented to monitor the postural stability of the biped. The simulation results reveal that the MHS possesses more sensitivity to change in overall height of the CM of the biped than the ZMP does; therefore, the MHS appropriately warns that foot rotation is approaching before it really happens since a manoeuvre starts.

II. BASIC CONCEPTS

The loss of postural stability may occur in several ways such as pure sliding, pure rotation, or combined sliding and rotation around one boundary edge of the support polygon of a biped. In this paper, the case of pure rotation is of interest, and it is assumed that the feet do not slip during bipedal locomotion. Moreover, this paper focuses on foot rotation during the single-support phase, during which all postural instabilities practically happen.

The MHS measure is defined based on stabilizing and destabilizing moments which are exerted to the edges of the supporting foot. A simple planar inverted pendulum attached to a rectangular base is considered as a simple model, representing the biped, shown in Fig.1. The boundary of the supporting polygon of the simple model is AB. To explain the MHS measure, the whole biped is firstly divided into two subsystems i.e. the foot and the shank. The net moment around the front and rear edges of the boundary of the supporting foot i.e. A and B are written as follows:

$$M_A = f_x d_1 + (f_y + m_f g) d_2 - \tau \tag{1}$$

$$M_B = f_x d_1 - (f_y + m_f g) d_3 - \tau \tag{2}$$

where M_A and M_B are the moment around the edges A and B, respectively. m_f is the mass of the foot; f_x and f_y are the horizontal and vertical components of the internal force at the ankle; τ is the internal torque at the ankle. g is gravitational acceleration that is constant, $9.81 \ \frac{m}{s^2}$. d_1, d_2, and d_3 are the height of the ankle, the posterior and the

anterior part of the foot, respectively. It is also assumed that the ankle and the foot CM are coincident.

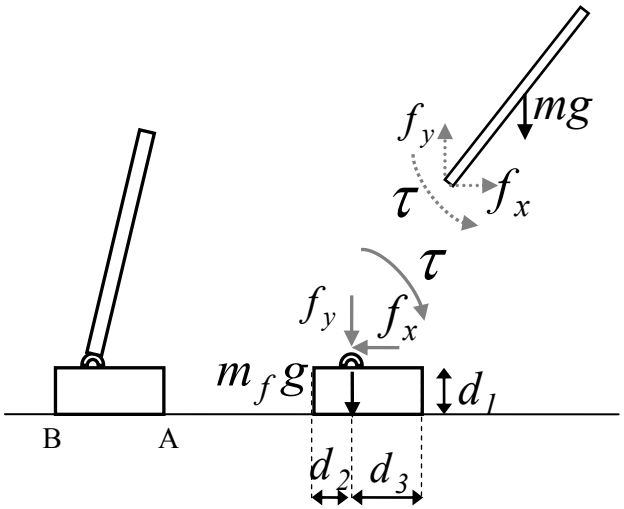

Fig. 1. A simple planar inverted pendulum model of the biped.

The positive direction of moment is counter clockwise. As shown in Fig. 2, if $M_A > 0$ and $M_B < 0$, the postural stability is guaranteed, and the foot will not rotate. If $M_A < 0$, the foot goes unstable and rotates around the front edge i.e. A, and if $M_B > 0$, the foot becomes unstable and rotates around the rear edge i.e. B.

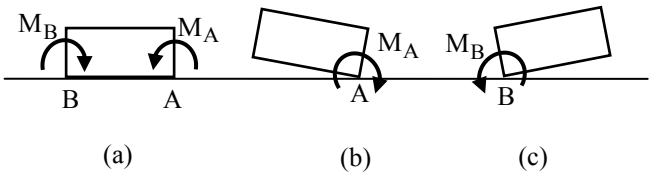

Fig. 2. The schematic of stabilizing and destabilizing Moments around the edges of the supporting foot.

If the foot is in contact with a sloped surface or an uneven terrain, the above statements will still be valid.

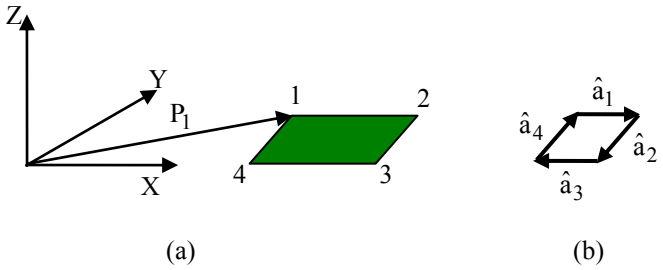

Fig. 3. The boundary of the supporting foot for a biped walking in 3D space.

III. MOMENT-HEIGHT STABILITY MEASURE

In this section, the MHS measure is applied to a general support polygon, shown in Fig. 3a. The following steps should be considered to apply the MHS measure. First, the biped is divided into two subsystems i.e. the supporting foot and the rest of parts of the biped. Next, all forces and torques exerted to the supporting foot are considered at the ankle joint. Those forces and torques are coming from the dynamics of the rest of parts of the biped, consisting of gravitational, inertial, and external forces and torques. The resultant moment around each edge of the supporting foot is calculated. These moments about edges *12*, *23* … and *n1* are named as $M_1, M_2, ..., M_n$, respectively.

After that, for each edge of the support foot, a unit vector $\hat{a}_i$ is defined such that the entire unit vectors make a closed loop direction in the clockwise direction when it is observed from above as shown in Fig. 3b. Since $P_1, P_2, ..., P_n$ represent the coordinate of contact points on the ground, the unit vectors of the support foot are computed as follows:

$$\hat{a}_i = \frac{P_{i+1} - P_i}{\|P_{i+1} - P_i\|} \qquad i = \{1, 2, ..., n-1\} \tag{3a}$$

$$\hat{a}_n = \frac{P_1 - P_n}{\|P_1 - P_n\|} \tag{3b}$$

Next, the dynamic MHS measure, α , is computed as follows:

$$\alpha = min(\alpha_i) \qquad i = \{1,2,...,n\} \tag{4}$$

Where α_i denotes the dynamic stability margin around the *i*-th boundary edge and is computed as:

$$\alpha_i = (I_{sf})^{\sigma_i}.(M_{v_i}) \qquad i = \{1,2,...,n\} \tag{5a}$$

$$M_{v_i} = M_i.\hat{a}_i \qquad i = \{1,2,...,n\} \tag{5b}$$

Where, I_{sf} , is the foot's moment of inertia around the *i*-th edge of the supporting foot, and σ_i is considered as:

$$\sigma_i = \begin{cases} +1 & ;if \quad M_{v_i} > 0 \\ -1 & ;Otherwise \end{cases} \quad i = \{1,2,...,n\} \tag{6}$$

Note that the inner product between the resultant moment M_i and $\hat{a}_i$ (unit vector) implies that if the moment around the *i*-th edge is stabilizing then α_i will be positive and if it is destabilizing then it will be negative. When the minimum of all α_i 's named α , is positive, the system is stable, and conversely the negative value of α displays the severity of instability of the biped. The zero value of α represents the critical dynamic stability of the biped.

The MHS measure incorporates the mass moment of inertia of the supporting foot, which

has significant effect on the possibility of foot rotation. For a stable case, the higher I_{sf} provides the more secure stability. On the other hand, for an unstable case, the higher I_{sf} provides slower rotation, and consequently the chance for stability compensation is greater.

The effects of stabilizing and destabilizing moments on the MHS, which has already been addressed, can still be improved. More specifically, the MHS measure in the above form is not directly explicitly sensitive to the height of the CM of the biped as shown in the Fig. 5b. The higher CM causes easier turning over, the MHS measure should be improved to be explicitly sensitive to the CM height of the biped:

$$\alpha = (h_{c.m.})^{\lambda}.min(\alpha_i) \qquad i = \{1,2,...,n\} \tag{7}$$

$$\lambda = \begin{cases} -1 & ;if \quad min(\alpha_i) > 0 \\ +1 & Otherwise \end{cases} \tag{8}$$

where, $h_{c.m}$ denotes the CM height of the biped. To compare the MHS measure and other postural stability measures, the following normalizing procedure is provided:

$$\hat{\alpha} = \frac{(h_{c.m.})^{\lambda}}{((h_{c.m.})_{nom})^{\lambda_{nom}}} \frac{(min(\alpha_i))}{(min(\alpha_i))_{nom}} \quad i = \{1,2,\ldots,n\} \tag{9}$$

where, $\hat{\alpha}$ is the normalized dynamic stability margin and subscript "nom" refers to the most stable posture of the biped. Note that the proposed normalized measure indicates a relative stability state which does not specify an absolute value. It should be mentioned that although both the MHS and the ZMP measures are moment-based, but the new proposed MHS measure is more effectual in two aspects as follows:

First, the ZMP does not indicate the severity of the biped's instability, [9], though it has been tried to be resolved by Vukobratovic in [7]. On the contrary, the proposed MHS indicates the severity of the biped's instability, such that the smaller α becomes, the higher the severity of instability will be. Second, in distinction to the ZMP, the MHS explicitly includes the CM height in order to monitor the postural stability of bipedal robots, as the CM height is very important for the case, in which heavy payloads are being manipulated.

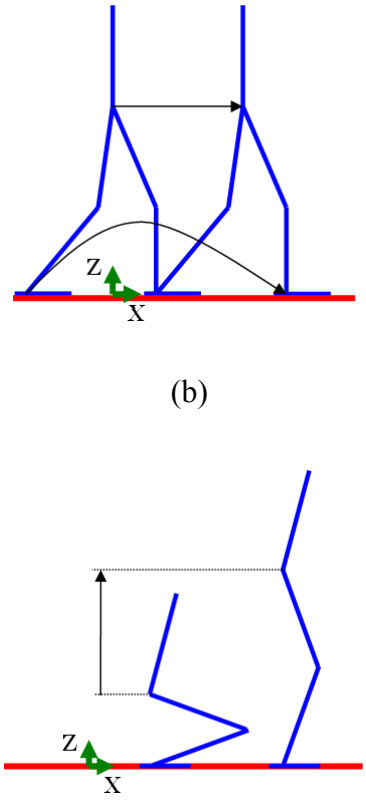

Fig. 4. Two types of biped manoeuvres, namely the standing up (a) and the swinging forward (b).

IV. CASE STUDIES

To compare the performance of the MHS measure with that of the ZMP measure, two cases of the biped manoeuvres are considered namely the standing up and the swinging forward. As shown in Fig. 4, the number of Degrees of Freedom (DOFs) of the biped is three and five during the standing up and the swinging forward, respectively. Table (I) illustrates the mass and geometrical parameters of the biped. At first, dynamically stable trajectories for the two types of manoeuvres are designed based on the ZMP criterion.

a. Trajectory Generation Based on the ZMP :

ZMP-based stable trajectories for the biped are achieved for both standing up and swinging forward phases by considering prescribed motion profiles for the lower body i.e. the hip and the ankle. The motion profile of the upper body is then computed to keep the biped stable [15-17]. The joint angular motion profiles of the biped are computed by the inverse kinematics equations [15].

Table I. The mass and geometrical parameters of the biped.

Upper body link	Lower body link
m_0(kg) 10	$m_1,..., m_i$ (kg) 1
I_0(kg.m^2) 0.208	$I_1,..., I_i$ (kg.m^2) 0.021
L_0(m)	$L_1,..., L_i$ (m)

0.5	0.5

In order to get rid of highly nonlinear multi-link dynamics of the biped, it is simplified to an inverted pendulum model (IPM), depicted in Fig. 5. The IPM is a simple representative of the biped CM, so solving its dynamic equation provides the CM trajectory of the biped.

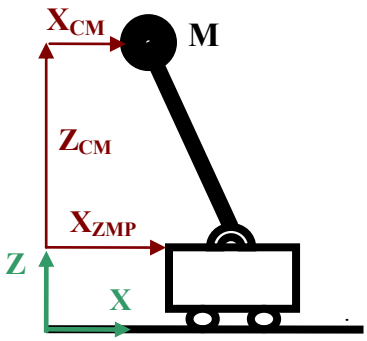

Fig. 5. The inverted pendulum model representing the biped.

It is noteworthy that in Fig. 5, the mass of the IPM is equivalent to the biped's total mass, and the pivot point of the pendulum is equivalent to the biped's ZMP. The wheeled rover at the base of the pendulum indicates that the ZMP could be assumed either fixed or moving [16]. Referring to the ZMP concept [7] and the above assumptions, the equation of motion for the IPM is obtained as follows:

$$\ddot{X}_{CM} Y_{CM} + (\ddot{Y}_{CM} + g)(X_{CM} - X_{ZMP}) = 0 \qquad (10)$$

where X_{CM} and Z_{CM} denote the position of the biped CM and X_{ZMP} denotes the x-component of the biped ZMP position. It is noteworthy that X_{ZMP} is regarded as a desired input for the above equation. Determined the desired ZMP for the IPM, the CM constraint is obtained solving the Eq. 10. The upper body motion is obtained via fulfilling the CM constraint since the lower body motion was already prescribed. Using Inverse Kinematics equations, the joint angular motion profiles of the biped are obtained. The ZMP of the biped, named the computed ZMP, is obtained, applying the designed trajectories for the hip, the ankle, and the trunk. To assure that the gait planning procedure

is reliable, the deviation of the desired ZMP and the computed ZMP should stay small within the support polygon of the biped.

Figs. 6 and 7 compare the desired ZMP for the IPM with that computed for the biped. As shown in Figs. 6 and 7, the desired ZMP for the standing up and the swinging forward cases are considered as fixed and moving, respectively. Figs. 6 and 7 show that the IPM is a reliable representative for the biped as the deviation between the desired ZMP and the computed ZMP is very small within the support polygon. The displacement of the biped's CM is obtained solving Eq. 10, considered as the CM constraint. The constraint is fulfilled via the upper body motion i.e. the trunk.

b. The MHS measure versus the ZMP Measure:

This section presents a comparison between the MHS and the ZMP. First, both metrics are normalized to the most stable pose, which is the middle of support polygon. Fig. 8 shows the MHS associated with the rear and the front stance foot edges, and also the minimum of them which reflect the overall stability status of the biped, described in Eqs. 5-7. The responses of the normalized ZMP and that of the MHS are very close to each other during the swinging forward phase, as it can be seen in Fig. 9. In distinction to the swinging forward phase, during the standing up phase, Fig. 10 and Fig. 11 demonstrate that the MHS response is distinguishable from the ZMP's since the MHS measure is explicitly defined sensitive to the biped CM height.

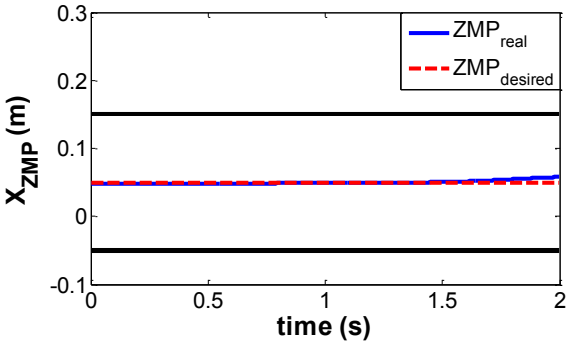

Fig. 6. Comparison the computed ZMP with the desired ZMP during the standing up phase.

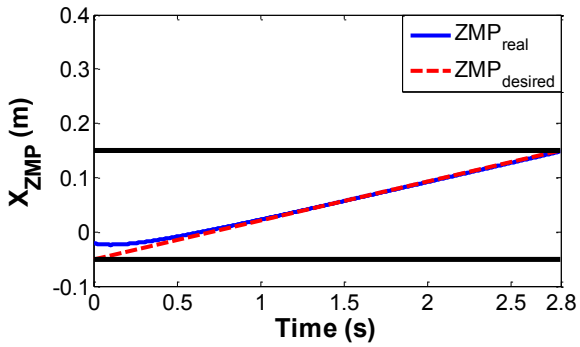

Fig. 7. Comparison the computed ZMP with the desired ZMP during the swinging forward phase.

The MHS is sensitive to the biped configuration especially once the biped is merely experiencing gravitational force, which may occur during the static or quasi static state of the biped heavy object manipulation. Fig. 12 also shows an animated view of the standing up phase. It is very important to point out that when the CM height of the biped elevates, the severity of postural instability will increase such that the opportunity for tip-over recovery will be reduced due to an impressed disturbance.

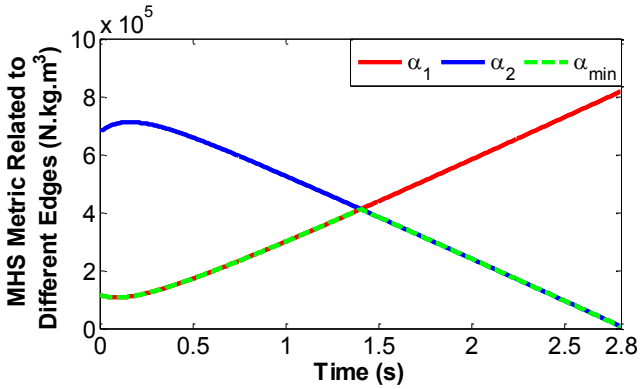

Fig. 8. The MHS measure related to the different edges of the support polygon during the swinging forward phase.

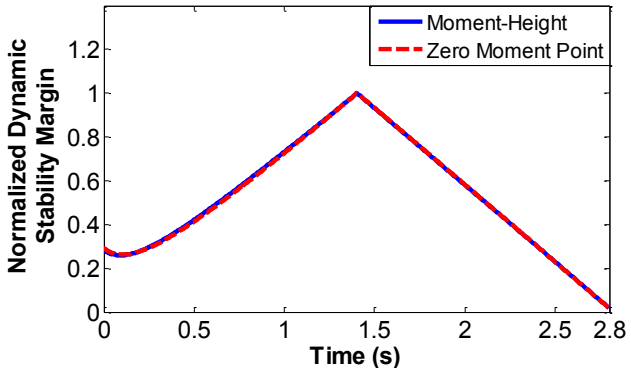

Fig. 9. Comparison between the MHS measure and the ZMP during the swinging forward phase.

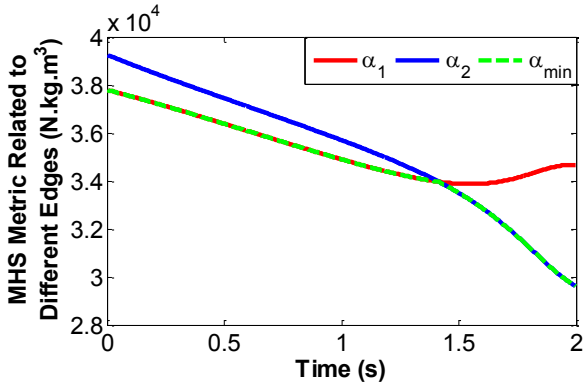

Fig. 10. The MHS measure related to the different edges of the support polygon during the standing up phase.

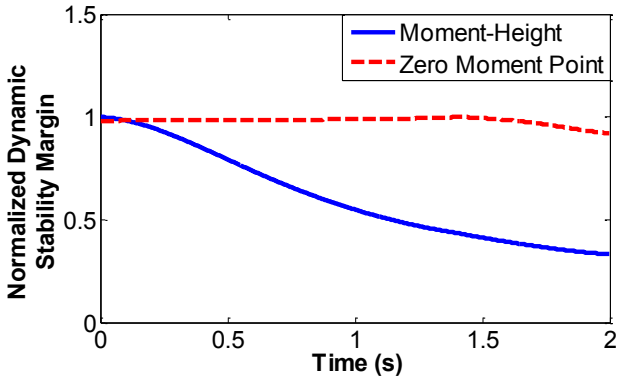

Fig. 11. Comparison between the MHS measure and the ZMP during the standing up phase.

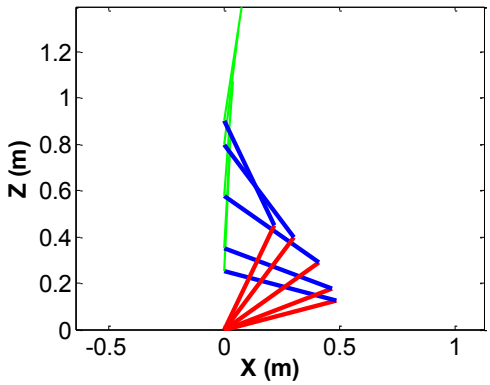

Fig. 12. The simulation of the biped robot during the standing up phase.

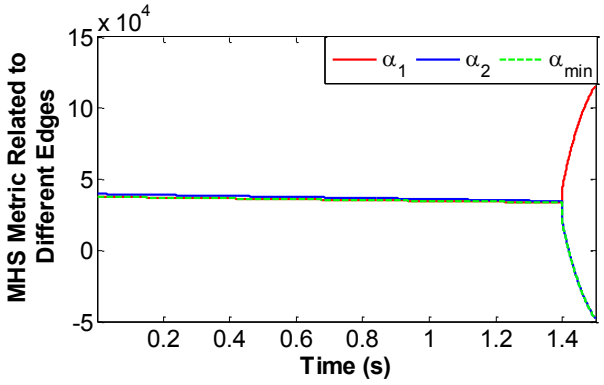

Fig. 13. The MHS measure related to different edges of the support polygon when the disturbance force (35N) exerted at the hip during the standing up phase.

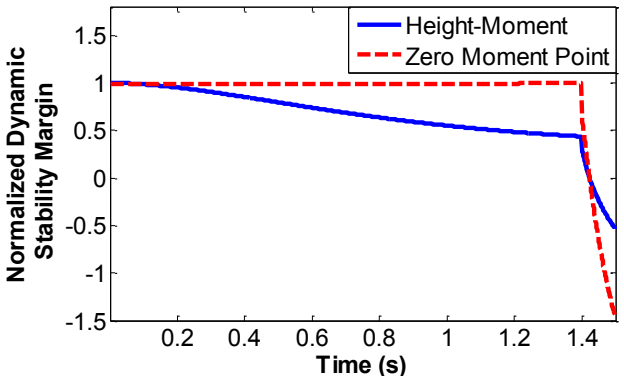

Fig. 14. Comparison between the MHS measure and the ZMP during falling down.

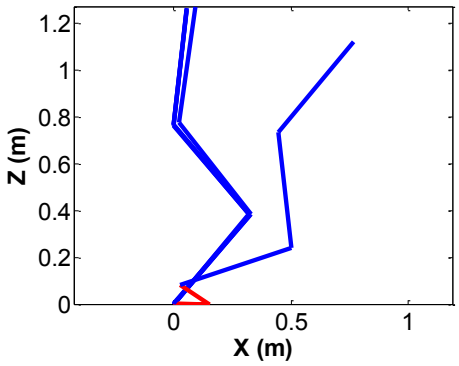

Fig. 15. The simulation of the biped robot during falling down.

As a result, this investigation reveals one drawback of the ZMP, that is, it does not alert the biped when the potential of postural instability amplifies during a quasi static manoeuvre. To highlight this fact, another case study is conducted in which the biped is subjected to a disturbing force exerting at the hip. The magnitude of this disturbance is $F_d = 35$ (N).

Note that in this case, the biped is simulated even after falling down, shown in Fig. 15. As it can be observed from Figs. 13 and 14, both measures (the MHS and the ZMP) predict the same tip-over instant of 1.4 (s). However, the MHS warns the biped that potential of instability is increasing from the start along the manoeuvre, while the ZMP alerts the biped immediately before falling happens, by which there is no time for push recovery.

V. CONCLUSION

In this paper a novel measure named as Moment-Height stability (MHS), which has been previously introduced by the authors for wheeled mobile robot, was exploited for the postural stability investigation of a planar biped. The proposed metric is physically meaningful based on principal concept and can be implemented with low computational effort. Two case studies were presented to compare the new MHS measure with the well known ZMP measure response which has been widely utilized in biped robot control as a postural stability metric. Simulation results proved the advantages of MHS over ZMP in terms of more sensitivity to the height of biped center mass. Simulation results were carried out to demonstrate the responses of both MHS and ZMP before and after fall. Note that in contrast to the ZMP, which does not provide any valid information before fall, the MHS metric indicates increasing the severity of instability from the start along the manoeuvre.

REFERENCES

[1] M. S. Nixon, T. Tan, and R. Chellappa, *Human Identification Based on Gait*. springer, 2006.

[2] M. Vukobratovic et al, *Biped Locomotion Dynamic, Stability, Control and Application*, springer-verlag 1990.

[3] S. Ali A. Moosavian, A. Takhmar, M. Alghooneh, “Regulated Sliding Mode Control of a Biped Robot”, *Proc. the International Conference on Mechatronics and Automation (ICMA 2007)*, China, pp. 1547-1552, 2007.

[4] P. Vadakkepat and Dip Goswami. "Biped Locomotion: Stability, Analysis and Control", *Int. Journal of Smart Sensing and Intelligent Systems*, Vol. 1, No. 1, pp. 187-207, 2008.

[5] M. B. Popovic, A. Goswami and H. Herr, “Ground Reference Points in Legged Locomotion: Definitions, Biological Trajectories and Control Implications*,” Int. Journal of Robotics Research*, Vol. 24, No. 12, pp. 1013-1032, 2005.

[6] M. Vukobratovic, A. A. Frank, and D. Jricic, “On the Stability of Biped Locomotion,” *IEEE Trans. On Biomedical Engineering*, Vol. 17 No.1, pp. 25-36, 1970.

[7] M. Vukobratovic, & B. Borovac, Zero moment point: Thirty five years of its life, *International Journal of Humanoid Robotics*, Vol. 1, No. 1, pp. 157-173, 2004.

[8] C. Yin, and et al. “stability Maintenance of a Humanoid Robot under Disturbance with Fictitious Zero-Moment Point (FZMP)”, *Proc. IEEE RSJ,* pp. 3149-3156, 2005.

[9] A. Goswami, “Postural Stability of Biped robots and the Foot Rotation Indicator (FRI) Point,” *Int. Journal of Robotics Research*, Vol. 18, no. 6, pp. 523-533, 1999.

[10] M. Popovic, A. Hofmann, and H. Herr, “Zero spin angular momentum control: definition and applicability,” in *Proceedings of the IEEE RAS/RSJ International Conference on Humanoid Robots*, pp. 478-493, 2004.

[11] A. Goswami and V. Kallem, “Rate of change of angular momentum and balance maintenance of biped robots” *Proc. of the IEEE Int. Conf. on Robotics and Automation*, pp. 3785-3790, 2004.

[12] Ali. A. Moosavian and K. Alipour, “On the Dynamic Tip-over Stability of Wheeled Mobile Manipulators,” *International Journal of Robotics and Automation*, Vol. 22, No. 4, pp. 322-328, 2007.

[13] S. Ali. A. Moosavian, K. Alipour, and Y. Bahramzadeh, "Dynamics Modeling and Tip-Over Stability of Suspended Wheeled Mobile Robots with Multiple Arms," *Proc. the IEEE/RSJ International Conference on Intelligent Robots and Systems*, USA, pp. 1210-1215, 2007.

[14] K. Alipour, and S. Ali. A. Moosavian, “Point-to-Point Stable Motion Planning of Wheeled Robots with Multiple Arms for Heavy Object Manipulation,” *Proc. Of the IEEE Int. Conf. On Robotics & Automation*, pp. 6162-6167, 2011.

[15] S. Ali A. Moosavian, M. Alghooneh, A. Takhmar, “Modified Transpose Jacobian Control of a Biped Robot”, *Proc. IEEE-RAS 7th International Conference on Humanoid Robots,* Pittsburgh, Pennsylvania, USA, pp. 282 - 287, 2007.

[16] S. Ali A. Moosavian, M. Alghooneh, A. Takhmar, “Cartesian Approach for Gait Planning and Control of Biped Robots on Irregular Surfaces,” *International Journal of Humanoid Robotics*, Vol. 6, No. 4, pp. 675-697, 2009.

[17] Q. Li, A. Takanishi, and I. Kato, “Learning control for a biped walking robot with a trunk,” *in IEEE/RSJ International Conference on Intelligent Robots and Systems*, vol. 3, pp. 1771-1777, 1993.

Mansoor Alghooneh, Amir Takhmar, and S. Ali. A. Moosavian, Monitoring the Postural Stability of Planar Bipedal Robots using the Moment-Height Stability Measure